Available online at www.sciencedirect.com
SCIENCE DIRECT®
ELSEVIER
Nuclear Instruments and Methods in Physics Research B 235 (2005) 231–234
NIM B Beam Interactions with Materials & Atoms
www.elsevier.com/locate/nimb

Measurement of electron impact collisional excitation cross sections of Ni to Ga-Like Gold

M.J. May [a], P. Beiersdorfer [a,*], N. Jordan [a], J.H. Scofield [a], K.J. Reed [a], S.B. Hansen [a], K.B. Fournier [a], M.F. Gu [b], G.V. Brown [c], F.S. Porter [d], R. Kelley [d], C.A. Kilbourne [d], K.R. Boyce [d]

[a] *Lawrence Livermore National Laboratory, L-260, Livermore, CA 94550, USA*
[b] *Stanford University, Stanford, CA 94305, USA*
[c] *Department of Physics and Astronomy, The Johns Hopkins University, Baltimore, MD 21218, USA*
[d] *NASA-Goddard Space Flight Center, Code 662, Greenbelt, MD 20700, USA*

Available online 26 April 2005

Abstract

We are measuring the cross sections for the 3d → 4f and 3d → 5f excitations in Ni- to Ga-like Au in beam plasmas created in the Livermore electron beam ion trap EBIT-I. The measurements are possible by using the high-resolution broadband coverage of the Goddard Space Flight Center micro-calorimeter. The cross sections are determined from the ratio of the intensity of the collisionally excited lines to the intensity of the radiative recombination lines. The value of the excitation cross section of the $3d_{3/2} \rightarrow 5f_{5/2}$ transition in Au^{50+} (Cu-like) is presented and compared to distorted wave calculations.

PACS: 34.80.Kw; 32.30.Rj; 32.70.Fw

Keywords: Electron-impact excitation cross sections; Gold M-shell; Microcalorimeter; EBIT

1. Introduction

Accurate electron-impact excitation cross sections are needed for proper interpretation of the spectral emission of highly charged ions and utilizing spectral measurements for plasma diagnostics. The determination of the ionization balance for a given plasma temperature is especially sensitive to the values of the excitation cross sections used to correlate the intensity of a given line to the abundance of the corresponding ion species. Knowing the correct charge state distribution

* Corresponding author. Fax: +1 925 423 2302.
E-mail address: beiersdorfer@llnl.gov (P. Beiersdorfer).

0168-583X/$ - see front matter © 2005 Elsevier B.V. All rights reserved.
doi:10.1016/j.nimb.2005.03.179

(CSD) in turn is critical for understanding radiation levels, energy deposition, energy balance, etc. of high temperature plasmas. Two high density experiments with different plasma conditions have been done with the NOVA laser to determine the ionization balance of Au ($Z = 79$). Foord et al. [1] inferred the charge state distribution of a gold microdot heated to $T_e = 2.2$ keV in steady state. Glenzer et al. [2] measured the CSD of gold in a fusion hohlraum plasma with $T_e = 2.6$ keV, $n_e = 1.4 \times 10^{21}$ cm^{-3}, and a soft X-ray radiation temperature of 210 eV. The CSDs were inferred by comparing the measured 5f → 3d spectrum with atomic physics calculations using electron impact excitation cross sections from the Hebrew University Lawrence Livermore Atomic Code (HULLAC) [3]. The experimentally inferred CSDs were in reasonable agreement with the modeled values from RIGEL [4]. However, the analysis was complicated by the transient nature of the laser produced plasma and the many competing atomic processes.

A CSD of gold was determined at low density ($\sim 10^{12}$ cm^{-3}) in a plasma with an electron temperature of 2.5 keV [5]. The plasma was created at the Livermore electron beam ion trap EBIT-II. The charge balance was inferred by fitting the observed 5f → 3d spectrum with modeled spectrum from HULLAC in a method similar to that done in the Nova experiments. Despite the relatively simple atomic physics in the low density EBIT-II plasma, significant differences existed between the experimentally inferred CSD and the simulations from several available codes.

Because inaccuracies in the calculated cross sections will introduce errors in the inferred CSD, the question arises how good are the calculated excitation cross sections and how large are the uncertainties. Accurate measurements of the cross sections will reduce this uncertainty. To this end, we have started measurements of the cross sections for the 3d → 4f and 3d → 5f excitations in Ni- to Ga-like Au from EBIT-I plasmas. Here we present the measurement of the $3d_{3/2} \rightarrow 5f_{5/2}$ transitions in Au^{50+} Cu-like. The experimentally determined cross sections are compared with the calculated cross sections from HULLAC, the Flexible Atomic Code (FAC) [6] and the Distorted Wave Code (DWS) [7].

2. Plasmas at the Livermore electron beam ion trap

The gold plasmas for the measurements were created in the Livermore electron beam ion trap EBIT-I [8,9]. Plasmas having a monoenergetic electron beam with energies, E_{beam}, of 2.92, 3.53 and 4.54 and 5.54 ± 0.04 keV were utilized for the cross section measurements. The electron beam had a Gaussian electron energy distribution with a full width half maximum of ≈50 eV. The data presented here were taken by using two different trapping cycles. The first had a single beam energy. The second started at a lower energy (e.g. 2.92 keV) for 43 ms and then switched to a higher energy (e.g. 5.54 keV) for 7 ms. The lower beam energy created the ions of interest. The higher beam energy excited the transitions necessary for the cross section measurements. Each trapping cycle condition was repeated continuously for 8 to 12 s before the trap was emptied. Each experimental condition required repeating the trapping cycle at the same conditions for ≈12 h to record sufficient signal in the weak radiative recombination (RR) emission. Details of the experimental conditions can be found in [5,10,11].

The GSFC microcalorimeter (XRS) [12,13] at Livermore recorded the collisionally excited gold lines from the 4f → 3d and 5f → 3d X-ray transitions between 2.0 and 4.0 keV and the RR features of Ni recombining into Cu, Cu recombining into Zn, etc., from 5.0 to 8.0 keV. A sample raw spectrum is shown in Fig. 1 for a plasma having $E_{beam} = 4.54$ keV. The XRS detector head consisted of an array of 30 active ion-implanted thermistors with a 8.5 μm thick HgTe photon absorber. The thermistors directly measured the temperature change of a single photon absorbed by the HgTe absorber which was cooled to 59 mK. The maximum count rate was limited to ≈100 counts per second across the entire array. The spectral resolution was ≈12 eV across the entire spectral range for these measurements.

3. Cross section calculations

HULLAC [3], FAC [6] and DWS [7] were used to calculate the electron impact collisional cross

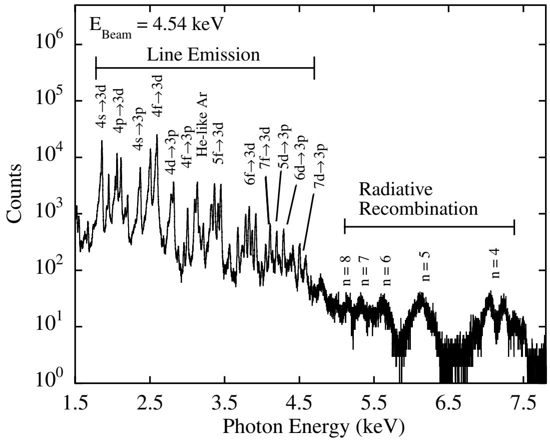

Fig. 1. Raw XRS spectrum in an EBIT-I plasma having an E_{beam} of 4.54 keV.

sections for the 3d → 4f and 3d → 5f excitations. HULLAC computed the energy level structure for each ion from the Dirac equation with a parametric potential. Total electron collisional excitation cross sections were calculated semi-relativistically in the distorted wave approximation. DWS calculated fully relativistic distorted wave cross sections and utilized the Dirac–Fock–Slater potential. FAC calculated cross section in the distorted wave using the factorization formula from HULLAC and a variant of the potential used by DWS. FAC and DWS provided the cross sections between the individual magnetic sub-levels. The cross sections calculated by the three codes for the Cu-like $3d_{3/2} \rightarrow 5f_{5/2}$ excitation are compared in Fig. 2. In general, the agreement was good between the total cross sections calculated by all three codes. The variations between the different calculations were 10–20%. The magnetic sub-level cross sections from FAC were in good agreement with DWS. The agreement between the cross sections for the 3d → 5f excitations were slightly better than those for the 3d → 4f excitations.

4. Collisional excitations cross section measurements

The total cross sections for the 3d → 4f and 3d → 5f excitations for Ni-like to Ga-like gold

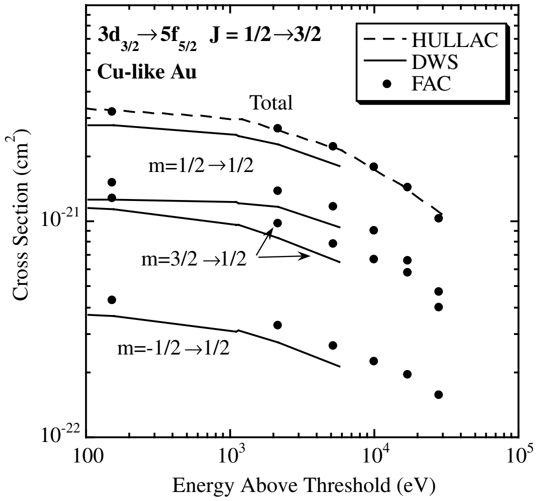

Fig. 2. Comparisons of calculated collisional impact cross sections for the $3d_{3/2} \rightarrow 5f_{5/2}$ Cu-like (Au^{50+}) excitations from HULLAC, DWS and FAC.

were determined from the intensities of the collisionally excited (CE) lines and RR emission recorded by the XRS. Details of the method can be found in [11,14]. The cross sections are related to the line and RR intensities by the formula

$$\sigma_{CE} = \frac{1}{B_{ai}} \frac{\sum_j G_j^{RR} \eta_j^{RR} T_j^{RR} \sigma_j^{RR}}{G^{CE} \eta^{CE} T^{CE}} \frac{I^{CE}}{I^{RR}}.$$

The sum, j, is over the fine structure levels. The intensities, I, are determined from the fits of the CE and RR features. The variables η and T are the XRS detector efficiency and filter transmissions, respectively. The variable B_{ai} is the branching ratio that accounts for autoionization. The CE lines and RR features from EBIT-I plasmas are polarized. The emission is viewed 90° from the direction of the beam. The polarization, P, is accounted for in the determination of the cross sections. The General Relativistic Atomic Structure Program (GRASP) [15,16] provided the RR cross sections that accounted for the polarization effects in EBIT-I and allowed simulation of the RR features for comparison with the measured spectra. For the line emission, the variable, G, is the angular distribution of the polarization, and $G = 3/(3 - P)$ for a dipole transition at 90°. The polarization is a function of the magnetic sublevel

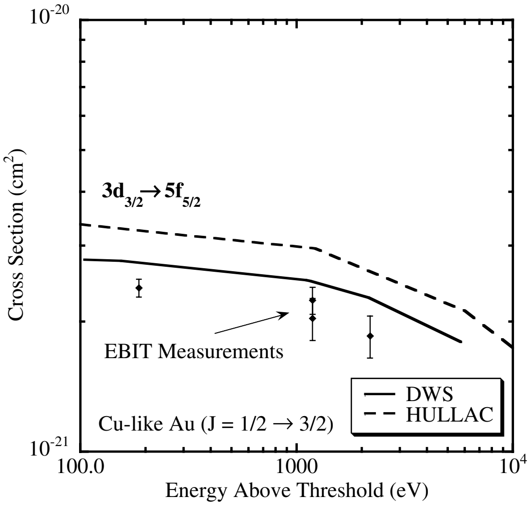

Fig. 3. Measured collisional excitation cross sections for the $3d_{3/2} \rightarrow 5f_{5/2}$ excitation in Cu-like (Au^{50+}) and comparisons to distorted wave calculations.

cross sections which were calculated by DWS. For the Ni-like $3d_{3/2} \rightarrow 5f_{5/2}$ excitation having $J = 0 \rightarrow 1$, $P = (\sigma_{-1} - 2\sigma_0 + \sigma_{+1})/(\sigma_{-1} + 2\sigma_0 + \sigma_{+1})$. The polarization is $\approx$0.3 at a $E_{\mathrm{Beam}} = 4.54$ keV.

The calculated total cross sections for the Cu-like (Au^{50+}) $3d_{3/2} \rightarrow 5f_{5/2}$ transition are compared with the measured values in Fig. 3. The points are the measured cross sections. The error bars on each point included the statistical error from the counts in the spectral line and RR features, the uncertainty in the fits to the line or RR features in each charge state, and the uncertainty in the XRS photometric calibration. The experimental cross sections are in good agreement with the calculations. Experimental cross section determinations are now in progress for the other transitions shown in Fig. 1. Preliminary results indicate that in some cases discrepancies with theory may be as large as 30%.

Acknowledgement

This work was performed under the auspices of the US DoE by the University of California Lawrence Livermore National Laboratory under contract W-7405-ENG-48.

References

[1] M.E. Foord, S.H. Glenzer, R.S. Thoe, K.L. Wong, K.B. Fournier, B.G. Wilson, P.T. Springer, Phys. Rev. Lett. 85 (2000) 992.

[2] S.H. Glenzer, K.B. Fournier, B.G. Wilson, R.W. Lee, L.J. Suter, Phys. Rev. Lett. 87 (2001) 045002.

[3] A. Bar-Shalom, M. Klapisch, J. Oreg, J. Quant. Spectrosc. Radiat. Transfer 71 (2001) 169.

[4] B.G. Wilson et al., in: W. Goldstein, C. Hooper, J. Gauthier, J. Seely, R. Lee (Eds.), Radiative Properties of Hot Dense Matter, World Scientific, Singapore, 1991.

[5] K.L. Wong, M.J. May, P. Beiersdorfer, K.B. Fournier, B. Wilson, G.V. Brown, P. Springer, P.A. Neill, C.L. Harris, Phys. Rev. Lett. 90 (2003), 235001-1.

[6] M.F. Gu, in: J.S. Cohen, S. Mazevet, D.P. Kilcrease (Eds.), Proceedings of the 14th APS Topical Conference on Atomic Processes in Plasmas, AIP Conf. Proc. No. 730 AIP, New York, 2004, p. 127.

[7] H.L. Zhang, D.H. Sampson, R.E.H. Clark, Phys. Rev. A 41 (1990) 198.

[8] R. Marrs, P. Beiersdorfer, D. Schneider, Phys. Today 47 (1994) 27.

[9] M.A. Levine, R.E. Marrs, J.R. Henderson, D.A. Knapp, M.B. Schneider, Phys. Scr. 22 (1988) 157.

[10] M.J. May, K.B. Fournier, P. Beiersdorfer, H. Chen, K.L. Wong, Phys. Rev. E 68 (2003) 036402.

[11] M.J. May et al., in: J.S. Cohen, S. Mazevet, D.P. Kilcrease (Eds.), Proceedings of the 14th APS Topical Conference on Atomic Processes in Plasmas, AIP Conf. Proc. No. 730 AIP, New York, 2004, p. 61.

[12] F.S. Porter et al., Proceedings SPIE 4140 (2000) 407.

[13] F.S. Porter et al., Rev. Sci. Instr. 75 (2004) 3772.

[14] H. Chen et al., Astrophys. J. 567 (2002) L169.

[15] F.A. Parpia, C.F. Fischer, I.P. Grant, Comput. Phys. Commun 94 (1996) 249.

[16] J.H. Scofield, Phys. Rev. A 9 (3) (1989) 3054.